

## FORCE/TORQUE SENSING AND MICRO-MOTION MANIPULATION OF A SPHERICAL STEPPING WRIST MOTOR

Kok-Meng Lee and Shankar Arjunan

Georgia Institute of Technology  
The George W. Woodruff School of Mechanical Engineering  
Atlanta, Georgia

### **ABSTRACT**

Recent developments in robotics and high precision manufacturing automation have provided the motivation for the re-examining of unusual designs of electromechanical transducers. This paper presents the coarse-fine motion strategy of the spherical stepper wrist motor which combines pitch, roll, and yaw motion in a single joint. By presenting the trade-off between the torque generated and the resolution for a realistic wrist motor design, the needs of a micro-motion mechanism as part of the spherical wrist motor are discussed. The design concept of a series-parallel actuated micro-motion mechanism to enhance the resolution and to provide an effective means of torque sensing is addressed. The micro-motion actuation is achieved by piezo-electric actuating devices which have relatively short response time and essentially infinite positioning resolution.

### 1. Introduction

Recent developments in robotics and data driven manufacturing have motivated a flurry of research activity in direct drives involving DC, stepping, and brushless electro-mechanical actuators to improve performance by eliminating backlash and friction due to gear meshing. These devices are normally employed to accomplish a single degree-of-freedom (DOF) motion. Hence, for a three DOF wrist joint, three single-axis motors are required. A spherical stepper wrist motor presents some attractive possibilities by combining pitch, roll, and yaw motion in a single joint [1]. Recently, a six DOF magnetically levitated variable compliance fine motion wrist has also reported in [2].

The goal is the creation of a spherical wrist actuator for precise isotropic wrist manipulation with built-in wrist force/torque sensing which was illustrated to be an effective means in force control and dynamic compensation of the unknown payload [3,4]. In addition to the compact design without the use of speed reducer, the spherical wrist stepper motor results in relatively simple joint kinematics and has no singularities in the middle of the workspace except at the boundaries. The significant potential in applications where the demand on workspace is low but high speed precision isotropic manipulation of end-effector orientation is required continuously in all directions provides an incentive for further development.

The theoretical basis of a field controlled spherical induction motor was performed in [5]. However, the realization of a prototype remains to be demonstrated. The mechanical design of a spherical induction motor is complex. Laminations are required to prevent movement of unwanted eddy currents. Complicated three phase windings must be mounted in recessed grooves in addition to the rolling supports for the rotor in a static configuration. These and other considerations lead to an investigation of alternative spherical actuators based on the principle of variable reluctance (VR) stepper motor [6]. The operation of the three DOF spherical stepper motor differs significantly from the single-axis stepper motor and thus presenting a challenge in the new design concepts of wrist sensing and micro-motion control.

The paper presents the coarse-fine motion strategy of the spherical stepper wrist actuator. By presenting the trade-off between the torque generated and the resolution for a realistic wrist motor design, the needs of a micro-motion mechanism are discussed. In particular, the design concept of a series-parallel actuated micro-motion mechanism to enhance the resolution and to provide an effective means of torque sensing is addressed.

### 2. Design Concepts

A conceptual schematic of a spherical electro-mechanical stepper motor with a series-parallel micro-motion mechanism is shown in Fig. 1. The micro-motion mechanism consists of a tripod-like in-parallel actuated mechanism [7] and a planar mechanism [8] in series. The tripod-like mechanism provides two orientation motions and one translatory motion in z-direction and the planar mechanism provides the x-y translational motions and a spin motion. The electro-mechanical wrist motor provides the coarse orientation control on the basis of variable reluctance principle. The micro-motion mechanism performs two basic functions in the wrist design; namely, micro-motion manipulation by piezo-electric actuating devices and wrist torque sensing.

**2.1 Spherical Stepper Wrist Motor:** The electro-mechanical stepper motor is made up of a hemispherical stator which houses the stator coils and a rotor which houses a set of permanent magnets. The rotor is supported freely by means of gimbals. The stator coils can be energized individually using a control

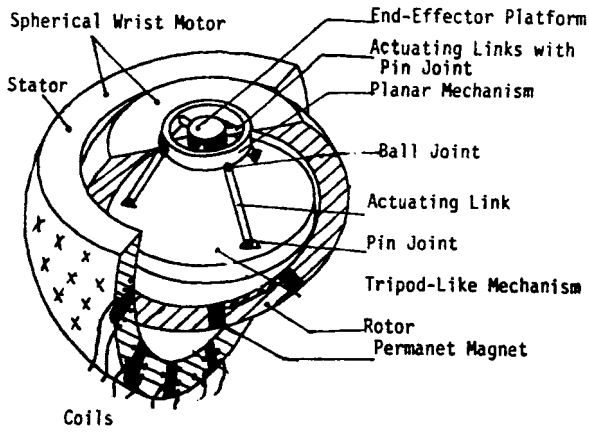


Fig. 1. Spherical Wrist Motor and Associated Mechanisms

circuity. As a pair of stator coils adjacent to the permanent magnets is energized, a magnetic field and a corresponding flux is generated. The tangential components of the magnetic force attract the adjacent magnets and hence exert a resultant torque on the rotor. Appropriate sequencing of high current pulses which excite the stator coils results in the rotor moving in any direction desired.

**Coil Arrangement:** The maximum number of coils which can be evenly inscribed on a spherical surface has been shown to be 20 based on the principle described by Pythagoras and Plato [6,9]. More than 20 coils are typically required in order to achieve a high positional resolution. A scheme, therefore, was devised to space the coils on the lower hemisphere of the stator as evenly as possible. The position of every coil is represented by the following mathematical relation. The inner surface of the stator is described by the spherical surface  $ST$ , radius  $r$ , and the coil positions is represented by an array of points,  $CP$ . The spacing between points is set by the angular parameter  $\theta$  which is in degrees and is positive.

$$ST = \{ (x,y,z) : x^2 + y^2 + z^2 = r^2 ; \\ Z \leq 0.0 \text{ and } x,y,z,r \in R \}$$

$$CP = \{ [(x,y,z), (i,j)] :$$

$$(x,y,z) \in ST \text{ and } i,j \in I \}$$

$$[(x,y,z), (i,j)] \in CP \text{ iff } x = r \sin(i\theta)$$

$$\text{and if } j = 0$$

$$\text{then } y = 0 \text{ and } z = -r \cos(i\theta)$$

$$\text{or if } j \neq 0$$

$$\text{there exist } \{(a,b,c), [i,j-\text{sgn}(j)]\} \in CP$$

$$\text{s.t. } (x,y,z) \cdot (a,b,c) = r^2 \cos \theta$$

**Wrist Torque Generation:** Unlike the conventional single-axis motor, the spherical actuator has an infinite number of rotational axes and has three degrees of freedom. With only one energized coil, a magnetic pole on the rotor surface can be actuated along any tangents on the inner surface of the stator and

thus allow two DOF motion control. The spin motion about an axis through the center of the rotor and the point of attraction can be provided by a second attraction between an additional active coil and a second permanent magnet. Hence, two forces which are not co-linear with the center of the rotor are necessary to provide spherical rotor stability at a static position and three DOF motion at any instant. Hence, in the following discussion, the restoring torque is based on a closed magnetic circuit consisting of two energized coils and a pair of permanent magnets. The closed circuit can be realized in practice by filling the rotor to a certain depth with iron trimmings and connecting the metallic cores of the coils by means of laminations.

As the stator coil positions and the permanent magnets are known with respect to the stator and rotor body frames respectively, the direction of the tangential force,  $F_i$ , can be determined using the homogenous transformation [A]. Hence, the restoring torque due to an active coil can be resolved with respect to the rotor body frame as :

$$T_i = P_i \times F_i \frac{(P_i - A^T Q_i)}{|P_i - A^T Q_i|} \quad (1)$$

and where  $P_i$  is the position vector of the center of the  $i^{\text{th}}$  magnet with respect to the rotor body frame;  $Q_i$  is the position vector of the center of the  $i^{\text{th}}$  coil with respect to the inertia frame; and  $F_i$  is the tangential force of  $i^{\text{th}}$  active coil under the influence of the magnetic system. The net restoring torque is the vector sum of the two torques generated and is dependent on the m.m.f. through the coils and the number of permanent magnet pairs.

**Wrist Motor Resolution:** It has been shown that the least number of attractions required to provide locking of the rotor is two. For a given pair of magnets, the arrangement of the stator coils described above determines the primary resolution, which is defined by the spacing of the coils. Further improvement in resolution can be achieved by increasing the number of magnet pairs or modifying the radius of the rotor.

The primary resolution of the spherical stepper motor depends on the spacing of the stator coils. The resolution of the stepper motor can be improved effectively by increasing the number of magnets. To facilitate the discussion, the definitions of phase and pole are introduced. A phase is defined as a set of coils which are turned on at the same instant in order to actuate or control the rotor at a specified orientation. As it has been shown previously at least two attraction points are necessary for mechanical stability, the minimum number of coils per phase is therefore two. A pole is defined as a set of permanent magnets which will be attracted by the active coils at a specified rotor orientation. Similarly, the minimum number of magnets per pole is two.

Hence, if there are  $N$  phases and one pole the rotor can be positioned at  $N$  specific orientations. To enable motion control in-between the discrete  $N$  specified orientations, additional phases or poles may be added corresponding to the desired positions on the inner stator surface or the rotor, respectively. The maximum number of desired discrete orientations is equal to the product of the number of phases and poles. To improve the resolution in a particular direction by a factor of two, for a given phase, two poles are necessary for  $2N$  desired discrete orientations in that direction. If the resolution in a second direction is to be double, the total number of desired discrete orientation is  $2^*(2N)$  or  $4N$ . In other words, three additional poles are required to improve the resolution by a factor of two in both directions. In general, it can be deduced that if the resolution of motion is to be improved by a factor of  $p$  times in  $q$  directions,  $(p^q - 1)$  additional poles are required for a given number of phases.

Alternatively, the resolution for a given number of poles can be improved by using micro-stepping scheme or by designing micro-toothed structure on the core and magnet surfaces.

**2.2 Micro-Motion manipulator:** Both resolution and restoring torque of the wrist motor depend on the number of primary magnetic systems. An increase in the number of primary magnetic circuits to improve the torque does not generally lead to an improvement in resolution. In fact, it is expected that the limited rotor surface area would result a in necessary trade-off between resolution and restoring torque obtainable. Hence, a micro-motion mechanism which consists of a spatial and a planar in-parallel actuated mechanisms is introduced to provide fine resolution in-between the discrete steps.

The detailed inverse kinematics of the tripod-like mechanism have been reported in [7]. The corresponding length of  $i^{\text{th}}$  link is :

$$|L_i| = \sqrt{(B_i - P_i) \cdot (B_i - P_i)} \quad (3)$$

where  $B_i$  and  $P_i$  are the position vectors of the ball and pin joints of  $i^{\text{th}}$  link with respect to the rotor body frame respectively. The link is constrained to move in a plane:

$$y_{B_i} = c_i x_{B_i} \quad (4)$$

where  $c_i$  has a numerical value of 0,  $\sqrt{3}$  or  $-\sqrt{3}$  corresponding to  $i = 1, 2,$  or  $3$  respectively. With a homogenous transformation matrix which specifies the end-point orientation/position, the link length is essentially a function of end-point orientation and position as :

$$L_i = L_i(\alpha, \beta, \gamma', x', y', z) \quad (5)$$

where  $\alpha, \beta,$  and  $\gamma'$  are the Z-Y-Z Euler angles and  $x', y',$  and  $z$  are the center of moving platform with respect to the rotor body frame. The corresponding constraint equations have been derived in [7] to be:

$$\gamma' = -\alpha \quad (6)$$

$$x' = -0.5 r (1 - \cos \beta) \cos 2\alpha \quad (7)$$

$$y' = 0.5 r (1 - \cos \beta) \sin 2\alpha \quad (8)$$

where  $r$  is the distance between the center of the moving platform and the ball joint.

Since the tripod-like mechanism has only three degrees of freedom, the planar mechanism is introduced to correct for the spin angle and the plane translations. For the specified position coordinates,  $x$  and  $y$ , and the spin angle,  $\gamma$ , with respect to the rotor body frame, the inverse kinematics of the planar mechanism can be shown to be :

$$\left. \begin{aligned} L_4^2 &= (r - r' \cos \Delta\gamma - \Delta x)^2 + (\Delta y + r \sin \Delta\gamma)^2 \\ L_5^2 &= \frac{1}{2} [(r' \cos \Delta\gamma + \sqrt{3} r' \sin \Delta\gamma - 2\Delta x - r)^2 + (\sqrt{3} r - 2\Delta y + r' \sin \Delta\gamma - \sqrt{3} r' \cos \Delta\gamma)^2] \\ L_6^2 &= \frac{1}{2} [(r' \cos \Delta\gamma - \sqrt{3} r' \sin \Delta\gamma - 2\Delta x - r)^2 + (-\sqrt{3} r - 2\Delta y + r' \sin \Delta\gamma - \sqrt{3} r' \cos \Delta\gamma)^2] \end{aligned} \right\} \quad (9)$$

where  $\Delta x = x - x', \Delta y = y - y'$  and  $\Delta\gamma = \gamma - \gamma'$

and where  $r'$  is the radius of the end-effector platform;  $\Delta x, \Delta y$  and  $\Delta\gamma$  are the corresponding plane position and the spin angle to be manipulated by the planar mechanism; and  $L_4, L_5$  and  $L_6$  are the link lengths of the planar mechanism.

For a given end-effector orientation  $(\alpha, \beta, \gamma)$  and cartesian position  $(x, y, z)$ , the actuating lengths of the mechanisms are calculated in two steps. First, the actuating lengths of the tripod-like mechanism are determined using Equation (3). As the actual  $x'$  and  $y'$  coordinates and the spin angle,  $\gamma'$ , of the moving platform are expressed in terms of the specified orientation,  $\alpha$  and  $\beta$ , in Equations (6)-(8), the actuating lengths of the planar mechanism can then be calculated using Equation (9). The simplicity of the inverse kinematics is an expected property of the in-parallel actuated mechanism.

### 3. Design of Micro-motion Manipulator

The prototype laboratory design of the tripod-like mechanism and planar mechanism are shown in Fig. 2 and Fig. 3 respectively. These mechanisms are composed of three independent links.

**3.1 Link Design:** For the tripod-like mechanism, each link is rigid except at the flexure springs indicated as point A and E in Fig 4. The flexure spring at A is designed so that the link can rotate about the point A which thereby behaves like a pin-joint and that at E is designed so that the platform mounted to the link can be rotated as a micro-motion ball joint. If the initial length is DE and its corresponding length under the

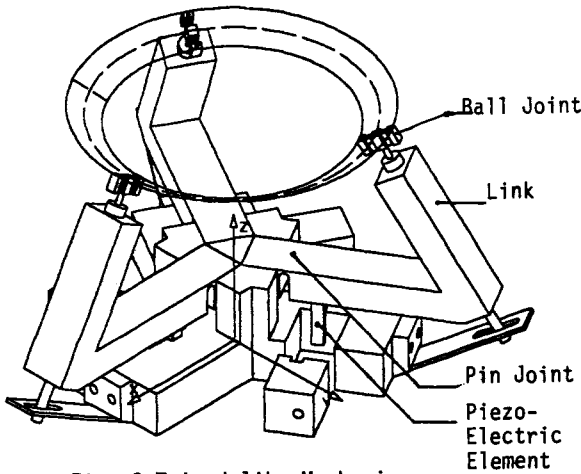


Fig. 2 Tripod-like Mechanism

action of external forces is  $DE'$ , conceptually one may visualize that the point  $D$  is a virtual pin joint and that the length  $DE'$  is a virtual actuating length,  $L$ . Hence, the effective change in link length is :

$$\Delta L = DE' - DE = DD' \sin \theta \quad (10)$$

The motion is caused by applying a positive electric potential to the rectangular-shaped piezo-electric actuating device which causes the material to strain axially. The axial strains result in displacements that cause the cantilevered beam to deflect. Deflection of the beam may be measured as electric potentials by the capacitance gauge or measured by means of strain gages. The cantilevered beam design enables the magnification of the strain to allow a larger working range and to increase the sensitivity of the strain measurement.

**3.2 Wrist Torque Sensing** The torque components to be sensed are that about the 1, 2 and 3 axes of the body frame fixed at the end-effector platform. However, as the motion of the mechanisms is of the order of microns which is very small compared to that of wrist motor, the force components to be sensed are viewed as that along the axes of the rotor body frame. Two torque components about the  $x$  and  $y$  axes and the force along the  $z$  axis are measured via the spatial mechanism. The spin torque and the forces along the  $x$ - and  $y$ - components are inferred from the measurements on the planar mechanism. Hence, the mechanism design must be such that the spatial mechanism is rigid in  $x$ ,  $y$  and  $z$  directions and the planar mechanism is rigid to external torques about  $x$ - and  $y$ - axes and to force along the  $z$ -axis.

For the tripod-like mechanism, the force and the torques to be measured are:

$$F_z = - \sum_{i=1}^3 F_{evi} \quad (11)$$

$$M_x = \sqrt{3} (F_{ev2} - F_{ev3}) \quad (12)$$

$$M_y = -F_{ev1} - \sqrt{3} (F_{ev2} + F_{ev3}) \quad (13)$$

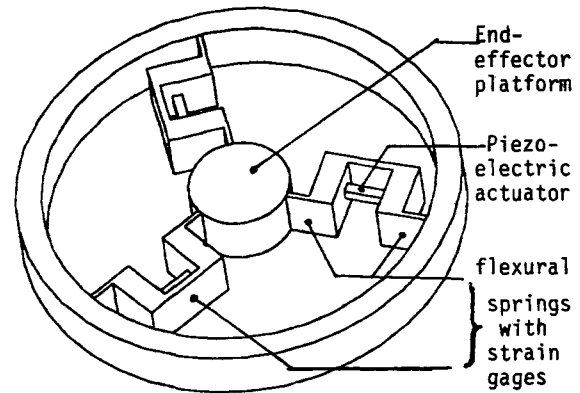


Fig. 3. Planar Mechanism

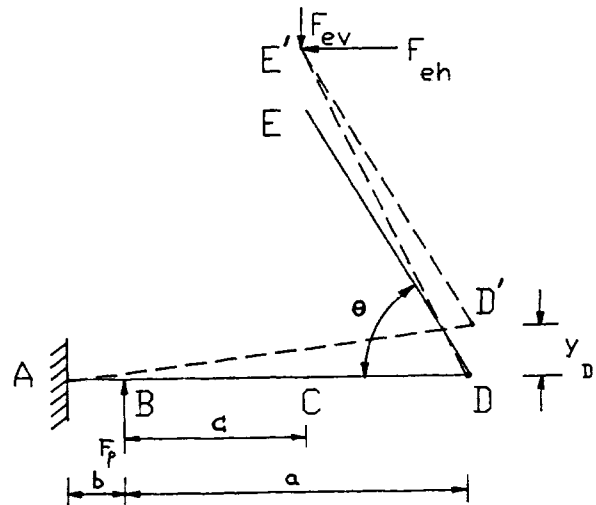


Fig. 4. Conceptual Schematic of Virtual Link

where

$$F_{evi} = \frac{6 y_{Di} EI - ab M_{Ai}}{c^2 - bc} \quad (14)$$

$$F_{pi} = \frac{6 y_{Di} EI - ac M_{Ai}}{b^2 - bc} \quad (15)$$

and where  $E$  and  $I$  are the modulus of elasticity and area moment of inertia respectively and the subscripts  $i$  ( $i = 1, 2, 3$ ) in  $F_{evi}$ ,  $F_{pi}$  and  $M_{Ai}$  refer to the  $i^{\text{th}}$  links respectively. Hence, by measuring the displacement  $y_{Di}$  and the net moment  $M_{Ai}$  of  $i^{\text{th}}$  link, the force and the torques can be determined from Equations (11)-(15).

For the planar mechanism, the tangential components of forces acting on end-effector platform result a spin moment. Also, the vector sum of the radial components yields the desired  $F_x$  and  $F_y$  respectively. The  $x$ - and  $y$ - force components and the spin torque can be determined by measuring the force components acting on the end-effector platform through the flexure spring which behaves as a pin joint.

#### 4. Micro-Motion Control

In the control of a manipulator, the end-point position and orientation are generally feedback by measuring the joint angles followed by forward kinematic computation. There are two difficulties encountered in the practical implementation as a result of this feedback scheme in the control of manipulator. (1) The forward kinematic of the in-parallel actuated mechanism is not in closed form and hence require tedious time-consuming numerical computation. (2) The feedback information is indirect and hence the static and dynamic effects of the manipulator on individual joint must normally accounted for using adaptive control scheme. In the micro-motion control, the first difficulty can be removed as the closed-form forward kinematic solution can be derived using standard linearization technique. The second difficulty can be overcome by considering the static and dynamic effects of the manipulator as the external forces/moments acting on the individual link, which are sensed and compensated.

In the control of the tripod-like or planar mechanism, the individual link is subjected to reaction forces at the ball joints, which must be compensated. The functional block diagram of the typical link control is shown in Fig. 5. For a specified position and orientation with respect to the rotor frame, the actuating length of each piezo-electric and hence the displacement at D can be determined using the inverse kinematic equations. Using the strain gages located at A and at D (indicated as gains  $K_1$  and  $K_2$  respectively), the external force components  $F_{ev}$  and  $F_{eh}$  can be sensed and compensated using feedforward control.

The piezo-electric actuated link dynamics were determined experimentally using the frequency response technique with an aid of HP signal analyzer. The parameters of the piezo-electric actuated link, as shown in Fig.4, are tabulated in Table 1. For the frequency range of 1000 Hz, the transfer function of the piezo-electric actuated link, which is a ratio of piezo-electric input voltage to the strain gage output at A, can be characterized by three pairs of complex poles and three pair of complex zeros which are tabulated in Table 1. The frequency response data are displayed in Fig. 6.

**TABLE 1 Piezo-electric Actuated Link Parameters**

**Piezo-electric elements:** TOKIN NLA 2x3x18[10]

**Aluminium link geometry:**

Cross section of link: 10.16mm x 13.5mm

Cross section of pin: 0.635mm x 13.5mm

a = 50mm, b = 5mm, c = 18mm,  $\theta = 60$  degrees

**Transfer Function:**

Poles: -8.7739 ± j 163.899

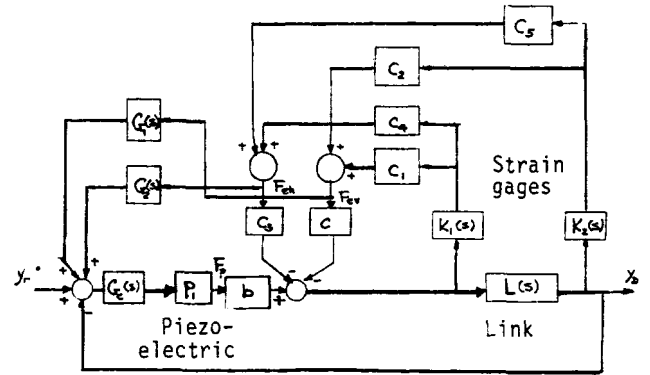
-41.320 ± j 489.184

-18.733 ± j 749.497

Zeros: -8.5471 ± j 223.446

-161.24 ± j 751.483

-79.812 ± j 1.2949k



b, c, c : geometric constants  
 $P_1$  : piezo-electric constant.

Fig. 5 Functional Block of Link Control

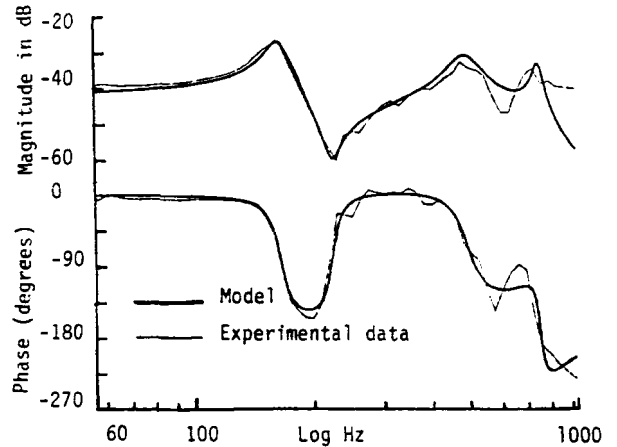


Fig. 6 Frequency Response of the Piezo-Electric Actuated Link

#### 5. Performance Prediction

It is of interest to predict the performance of the micro-motion mechanism and built-in torque sensor. A range of design parameters and their working range using piezo-electric material are listed in Table 2. The maximum travel and force generation of these piezo-electric materials are 10  $\mu\text{m}$  and 350  $\text{Kg/cm}^2$  respectively [10]. The maximum ranges of roll, pitch and spin angles are of the order of 1 degree. The ranges of x- and y-motion are in the order of 250  $\mu\text{m}$  and that of the z-motion is 60  $\mu\text{m}$ . Further increase of range of motion can be obtained by actuating piezo-electric materials in series.

A closed-loop step response was determined to predict the response time of the piezoelectric actuated link. A first order filter of 120 Hz to attenuate the high frequency components at the strain gage output was introduced. The closed loop position control of the piezo-electric actuated link using a PI controller was implemented digitally using QUICK BASIC (Version 4) on an IBM PC/XT. The sampling time of the control loop was limited to approximately 1 msec. Fig. 7 shows the experimental data and the model predictions. Approximately 8 msec of rise time was obtained. It is expected that the rise time can be further improved with reduced sampling time.

TABLE 2 Design Parameters

(a) Spatial mechanism

Radius of base platform = 0.0675m

Initial DE' (m)	$\rho$	Roll (deg) x-axis	Pitch(deg) y-axis	$\Delta z$ ( $\mu\text{m}$ )
0.055	0.6	0.81	1.80	60
0.081	0.4	1.03	2.11	60
0.108	0.2	1.46	2.99	60

\*  $\rho = \frac{\text{Radius of movable platform}}{\text{Radius of base platform}}$

(b) Planar mechanism

Radius of end-effector platform = 0.055m

Initial DE' (m)	$\rho^{**}$	$\Delta x$ ( $\mu\text{m}$ )	$\Delta y$ ( $\mu\text{m}$ )	$\Delta \gamma$ spin (deg.)
0.033	0.4	200	320	2.5
0.0275	0.5	240	240	2.5
0.022	0.6	280	280	1.5

\*\*  $\rho = \frac{\text{Radius of end-effector platform}}{\text{Radius of movable platform}}$

6. Conclusion

By presenting the trade-off between the restoring torque and the corresponding resolution for a realistic wrist motor design, the needs of a micro-motion mechanism have been discussed. The design concept of a series-parallel actuated micro-motion mechanism has been presented. The micro-motion actuation is achieved by piezo-electric device which is characterized by its short response time and essentially infinite resolution.

The emphasis of this paper was placed on the link design along with its associated force/position sensors to provide the overall wrist force/torque information. The closed-form inverse kinematics of the 6 DOF micro-motion mechanism which consists of a tripod-like spatial mechanism and a planar mechanism has been derived. An approach to micro-motion control has been suggested to overcome the difficulties associated with the end-point feedback of the micro-motion manipulator. Currently, work is underway to investigate the hysteresis effect of the piezo-electric actuating device on the link control. A prototype micro-motion mechanism is being built for experimental verification. Future work will focus on the design and control of the integrated spherical motor.

ACKNOWLEDGEMENT

Research work is supported by the General Research Fund of the School of Mechanical Engineering at Georgia Tech. The support of Graduate Research Assistant by the Computer Integrated Manufacturing Systems (CIMS) is gratefully acknowledged.

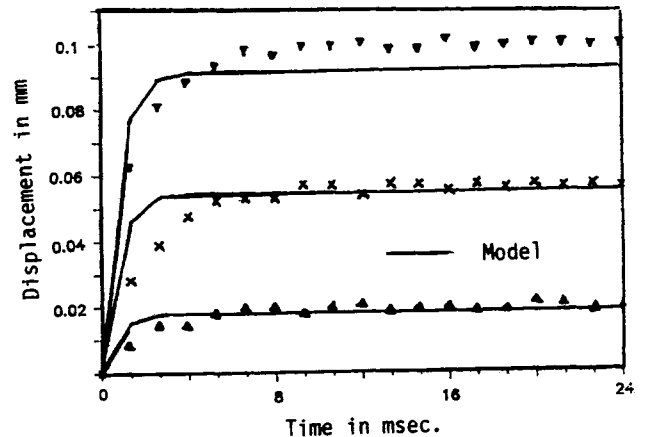


Fig. 7 Closed-loop Step Response

REFERENCES

- (1) Vachtsevanos, G.J., and Davey K., and Lee, K. "Development of a Novel Intelligent Robotic Manipulator," Control Systems Magazine, June 1987.
- (2) Hollis, R. L., Allan, A.P. and Salcudan, S., "A Six Degree-of-Freedom Magnetically Levitated Variable Compliance Fine Motion Wrist," The 4th Int'l Symp. on Robotics Research, Santa Cruz, August 1987.
- (3) Shimano, B. and Roth, B. "On Force Sensing Information and its use in Controlling Manipulators," Proceedings of the Eighth Industrial Symposium on Industrial Robots, Washington, D.C. Pages 119-126.
- (4) Raibert, M. H. and Craig, J. J., "Hybrid Position/Force Control of Manipulators," Trans. of ASME Journal of Dyn. Sys., Meas. and Control, Vol. 102, June 1981, Pages 126-133.
- (5) Davey K. and Vachtsevanos, G. "The analysis of Fields and Torques in a Spherical Induction motor," IEEE Trans. Mag., March 1987.
- (6) Lee, K-M., Vachtsevanos, G. and Kwan C-K., "Development of a Spherical Stepper Wrist Motor" Submitted to 1988 IEEE International Robotics and Automation. Philadelphia, April 25-29, 1988.
- (7) Lee, K-M and Shah, Dharmen, "Kinematic Analysis of a Three Degree of Freedom In-parallel Actuated Manipulator," Proceeding of the 1987 IEEE International Conference of Robotics and Automation, Raleigh. Also to be appeared in IEEE Journal of Robotics and Automation.
- (8) Powell, M. A. and Soni, A. H., "A Simulation Algorithm for a Three Legged Crawling Robot," 9th Applied Mechanisms Conference, Oct. 1985.
- (9) Smith, D. E., "Essentials of Plane and Solid Geometry," Wentworth-Smith Mathematical Series, 1923
- (10) Tokin Corporation, "Multilayer Piezo-electric Actuator," Vol. 01.